Histochemical Demonstration of an ATP-Dependent Ca^{2+}-Pump in Bullfrog Myocardial Cells

R. Meyer, W. Stockem, M. Schmitz

Institut für Cytologie, Universität Bonn, Ulrich-Haberland-Str. 61 A, D-5300 Bonn, Bundesrepublik Deutschland

and H. G. Haas

Institut für Physiologie II, Universität Bonn, D-5300 Bonn, Bundesrepublik Deutschland

Z. Naturforsch. **37 c**, 489–501 (1982); received February 5, 1982

Bullfrog Myocardium, Histochemistry, Freeze-Etching, Caveolae-System, Ca^{2+}-Pump

In the present investigation different finestructural and histochemical procedures were employed to demonstrate normal morphology and Ca^{2+}-transport mechanism in bullfrog atrial myocardium. For normal morphology specimens were fixed in 1% OsO_4, 2.5% glutaraldehyde or liquid propane at −185 °C before they were prepared for conventional embedding and freeze-etching, respectively. Special interest was focussed on the caveolae system, which is composed of single, spherical membrane invaginations (diameter, 85 nm), randomly distributed at the entire cell periphery. The caveolae enlarge the cell surface by 24.5% and occupy 8.5% of the cellular volume. The caveolae membrane contains a few intramembraneous particles with a diameter of 8.4 nm comparable to the size of ATPases as found in other cells.

For histochemistry the specimens were first stabilized by treatment with 50% glycerol, 0.025% glutaraldehyde or 0.15% formaldehyde and then incubated in a medium containing 4 mM $CaCl_2$, 4 mM EGTA, 5 mM $MgCl_2$, 5 mM $K_2C_2O_4$, 5 mM ATP and 20 mM histidine at pH 7.0. This incubation always succeeded in the formation of electron-dense deposits with elliptical shape, measuring 100–200 nm in length and 10–30 nm in diameter. According to X-ray spectra they deliver a characteristic calcium-peak and can be found within two different cellular compartments: in small invaginations of the sarcolemma, *i. e.* the caveolae-system, and in the intrafibrillar sarcoplasmic reticulum.

The elliptical deposits can be clearly distinguished from round electron-dense granules measuring 16 nm in diameter, which are located within randomly distributed small vesicles and composed of potassium and phosphate. Contrary to the elliptical deposits the round granules are also present in controls and seem to be identical with the so-called atrial granules.

In comparison to observations obtained with the same method in other muscular systems and derived from various control experiments the results of this study favour the existence of an ATP-dependent Ca^{2+}-pumping mechanism in frog atrial muscle bound to both, the sarcoplasmic reticulum and the caveolae system.

Introduction

Calcium plays an important role in the contraction-relaxation cycle of cardiac muscle cells. Increase and decrease of free cytoplasmic Ca^{2+} causes contraction and relaxation of the actomyosin system, respectively. Since the experiments of Ringer, carried out in the last century, it is generally accepted that a large share of Ca^{2+} necessary for contraction derives from the extracellular space. Later, it was shown that in skeletal muscle the sarcoplasmic reticulum (SR) is responsible for Ca^{2+}-regulation [1]. The importance of a SR for the electro-mechanical coupling of heart muscle cells, however, is still under discussion (reviewed by [2, 3]). Especially in amphibian heart muscle cells with a less developed SR than mammalian heart cells [4, 5], the involvement of this structure in Ca^{2+}-transport is obscure. Nevertheless, a Ca^{2+}-ATPase, comparable to the situation in skeletal muscle SR [6], generally exists in heart muscle SR, too [7]. Beside this a second Ca^{2+}-extrusion mechanism was described in heart muscle cells as Na^+/Ca^{2+} countertransport across the sarcolemma [8, 9]. For long this mechanism was considered to be the only possibility to transport Ca^{2+} across the myocardial sarcolemma. Recently, a third Ca^{2+}-transport system comparable to the Ca^{2+}-pump of the red blood cell plasma membrane [10] was detected in the sarcolemma of mammalian heart muscle cells [11] as well as in several other cell types, *e. g.* nerve cells [12] or lymphocytes [13]. In

Reprint requests to Prof. Dr. W. Stockem.

0341-0382/82/0500-0489 $ 01.30/0

amphibian heart muscle cells, however, indications for the localization of a Ca^{2+}-ATPase system bound to the sarcolemma or SR are not proved so far.

We therefore investigated the phenomenon of Ca^{2+}-transport in bullfrog atrial cells by means of histochemical methods to demonstrate ATP-dependent Ca^{2+}-accumulation in cytoplasmic compartments. As the sarcolemma of atrial cells has developed characteristic impocketings, *i.e.* the caveolae [14–16], special interest was focussed on the caveolae by investigating both, morphology and function of this system in ultrathin sections and freeze-etch replicas.

Materials and Methods

Muscle strips dissected from bullfrog (*Rana catesbeiana*) auricles in Ringer solution (111 mM NaCl, 5.4 mM KCl, 2 mM $CaCl_2$, 1.8 mM $KHCO_3$) were placed in a dish with paraffin bottom and attached to the ground with small needles to avoid contraction and changes in shape during fixation and dehydration.

For general morphology muscle strips were fixed with a mixture of 2.5% glutaraldehyde and 1% OsO_4 in 0.05 M cacodylate buffer (always pH 7.2) for 10 min [17], followed by 2.5% glutaraldehyde in the same buffer for 50 min. After removing the fixation media by washing in 0.05 M cacodylate (1 h), the specimens were postfixed for 1 h with 1% OsO_4 in 0.05 M cacodylate-buffer, dehydrated in a graded series of ethanols and embedded in Spurr's low viscosity resin [18]. For freeze-fracture studies muscle strips were fixed with glutaraldehyde and OsO_4 as described before or with 2.5% glutaraldehyde in 0.1 M PIPES-buffer (pH 7.2) for 1 h. The specimens were then washed in the same buffer for 30 min and transferred to a series of glycerol solutions (10%, 20%, 30%, 40%) at times of 30 min. Specimens taken from different final concentrations of glycerol (20%, 30%, 40%) were rapidly frozen in liquid propane cooled with liquid nitrogen. As controls living specimens were taken from Ringer solution and frozen natively in liquid propane by a cryojet (own construction). All probes were freeze-fractured in a Bioetch 2005 (Leybold-Heraeus + Co) apparatus at −100 °C, etched for 120 s at a vacuum pressure of about 10^{-7} mbar and shadow-casted with platinum/carbon ($\measuredangle 45°$) and carbon ($\measuredangle 90°$). Replicas were cleaned with 30% chromic acid and mounted on copper grids.

For histochemistry muscle strips were stabilized at 4 °C under conditions, which have proved not to destroy the activity of the sensitive extra ATPase especially in the presence of ATP [19]. The following procedures were used:

a) 0.025% glutaraldehyde in 14 mM veronal-acetate-buffer (pH 7.2) containing 5 mM ATP, 30 mM KCl, 5 mM $CaCl_2$ and 20 mM $MgCl_2$,
b) 0.15% paraformaldehyde in the same solution as described in (a). Afterwards the aldehydes were washed out by veronal-acetate-buffer containing all additives mentioned above (a) with the exception of ATP,
c) 50% glycerol in 0.5 M Tris-buffer (pH 7.2) containing 5 mM ATP, 30 mM KCl, 5 mM $CaCl_2$, 20 mM $MgCl_2$, 10 mM EGTA. Glycerol was removed by a graded series of decreasing glycerol concentrations with the same additives but without ATP.

During the procedures a–c the Na^+-concentration never exceeded 10 mM.

Subsequently all specimens were transferred to an incubation medium composed according to Heumann [20]: 4 mM $CaCl_2$, 4 mM EGTA, 5 mM $MgCl_2$, 5 mM $K_2C_2O_4$, 5 mM ATP, 20 mM histidine (pH 7.0). The incubation was carried out for 6 h at room temperature with solution exchange every 30 min.

For controls four different variations of the incubation medium were used:

a) Incubation medium without ATP;
b) incubation medium with 1 mM salyrgan;
c) incubation medium with 10^{-5} M ouabain;
d) incubation medium without ATP and with an addition of 150 mM NaCl.

After incubation all probes were washed with 14 mM veronal-acetate-buffer and postfixed with 2% OsO_4 in the same buffer. After washing with buffer and dehydration in a graded series of ethanols the specimens were finally embedded in Spurr's low viscosity epoxy resin. Up to 70% ethanol all solutions contained 10 mM $K_2C_2O_4$.

Ultrathin sections of the embedded materials were cut on LKB-microtomes. The probes for general morphology were stained with 0.5% uranyl acetate/70% ethanol for 30 min or 1% lead citrate in aqua bidest for 10 min.

Sections and replicas were observed with a Philips 200 electron microscope at 60 KV or with a Philips 301 electron microscope at 80 KV. Microanalysis was carried out with a Philips 300 electron microscope at 80 KV equipped with STEM-unit and EDAX-microprobe analysis.

Probes for X-ray microanalysis remained always unstained. Some probes were cut without floating the sections on water, *i.e.* dry to avoid solvation of ions.

Results

1. General morphology

Bullfrog atrial tissue consists of mononuclear cells with a diameter of 2–10 µm, which contain between one and four myofibrils. Intercalated discs are lacking and cells are connected with each other by desmosomes (cardiac adhesion plaques, [21] and gap junctions. The nucleus is surrounded by a metabolic center including mitochondria, dictyosomes, atrial granules and other cell organelles. Outside this center mitochondria are also present in discontinous rows along the myofibrils (Fig. 1 b). A sarcoplasmic reticulum is infrequent and usually not very prominent from the morphological point of view (Fig. 2 c). Only after weak fixation for histochemical experiments it appears swollen and becomes clearly visible (Fig. 3 c, 4 a and b).

As far as known a characteristic *t*-system is lacking in frog atrial cells. However, along the intire cell surface the plasma membrane forms numerous small spherical membrane invaginations (caveolae), which are visible in both, freeze-etch replicas (Fig. 1 a, c, 2 a, b) and ultrathin sections (Fig. 1 b). In freeze-etch replicas two structural aspects are prevailing: (a) cross-fractures through the plasma membrane (Fig. 1 c, 2 a, b) showing either EF (arrow-heads in Fig. 1 c, 2 b) or PF (arrows in Fig. 1 c, 2 b and Fig. 2 a) of the invaginations and (b) flat-fractures through the hydrophobic layer of the plasma membrane (Fig. 1 a, 2 b, star) showing the caveolae cross-fractured at the level of their necks, *i.e.* they appear as depressions in PF (Fig. 1 a, Inset, 2 b, white arrow-heads) and as prominent structures in EF of the plasma membrane.

To estimate the number of caveolae per unit of cell surface and calculate the membrane enlargement caused by these invaginations their openings were counted in replicas of flat-fractured plasma membrane (compare Fig. 1 a). Altogether, an area of 600 μm^2 containing 6682 caveolae was evaluated taken from several preparations after different pretreatments. The evalution yielded an average density of 10.8 caveolae/μm^2 (SD ± 2.73). The mean diameter of single caveolae measured in both, fracture faces and ultrathin cross-sections was 85 nm (SD ± 25.9; $n = 84$). On the assumption that most caveolae are spherical this diameter implies an average surface area of 0.0227 μm^2 per invagination. Considering the number of caveolae per μm^2 (10.8 ± 2.73) the surface of bullfrog atrial cells is enlarged by the caveolae invagination system by 24.5%. The measured diameter of an atrial myocardial cell varies between about 10 µm in the region of the nucleus and 4–6 µm at the other areas except the tips ([22, 23], own measurements). Assuming that such a cell is cylindrical with an average diameter of 5 µm the volume of the caveolae is 8.75% of the total cell volume.

The density of intramembraneous particles (IMP) on the EF and PF of the caveolae is distinctly lower than the IMP-density on corresponding faces of the residual plasma membrane. The diameter of the IMP in caveolae membranes is 8.4 nm (SD ± 2.0) compared to the diameter of IMP in the plasma membrane 5.4 nm (SD ± 2.6).

2. Histochemistry

The stabilization media used for histochemical demonstration of an ATP-dependent Ca^{2+}-pumping system contained aldehydes in very low concentration and hence resulted in a reduced preservation-quality of the tissue (Fig. 3 a, 4 a, c, 5 a). While myofibrils and nuclei exhibit a rather normal morphology, mitochondria and parts of the endoplasmic reticulum appear partly swollen and destroyed (Fig. 4 a). Similar observations were made after application of glycerol instead of aldehydes for cell dehydration and stabilization (Fig. 3 b, c, 4 b, d, 5 b).

In spite of the reduced fine structural preservation all specimens incubated according to the method of Heumann [20] (see materials and methods) reveal a large number of electron dense deposits within various cellular compartments (Figs. 3–5). Two types of deposits can be distinguished with regard to their shape, cellular localization and molecular composition: (a) Membrane-surrounded

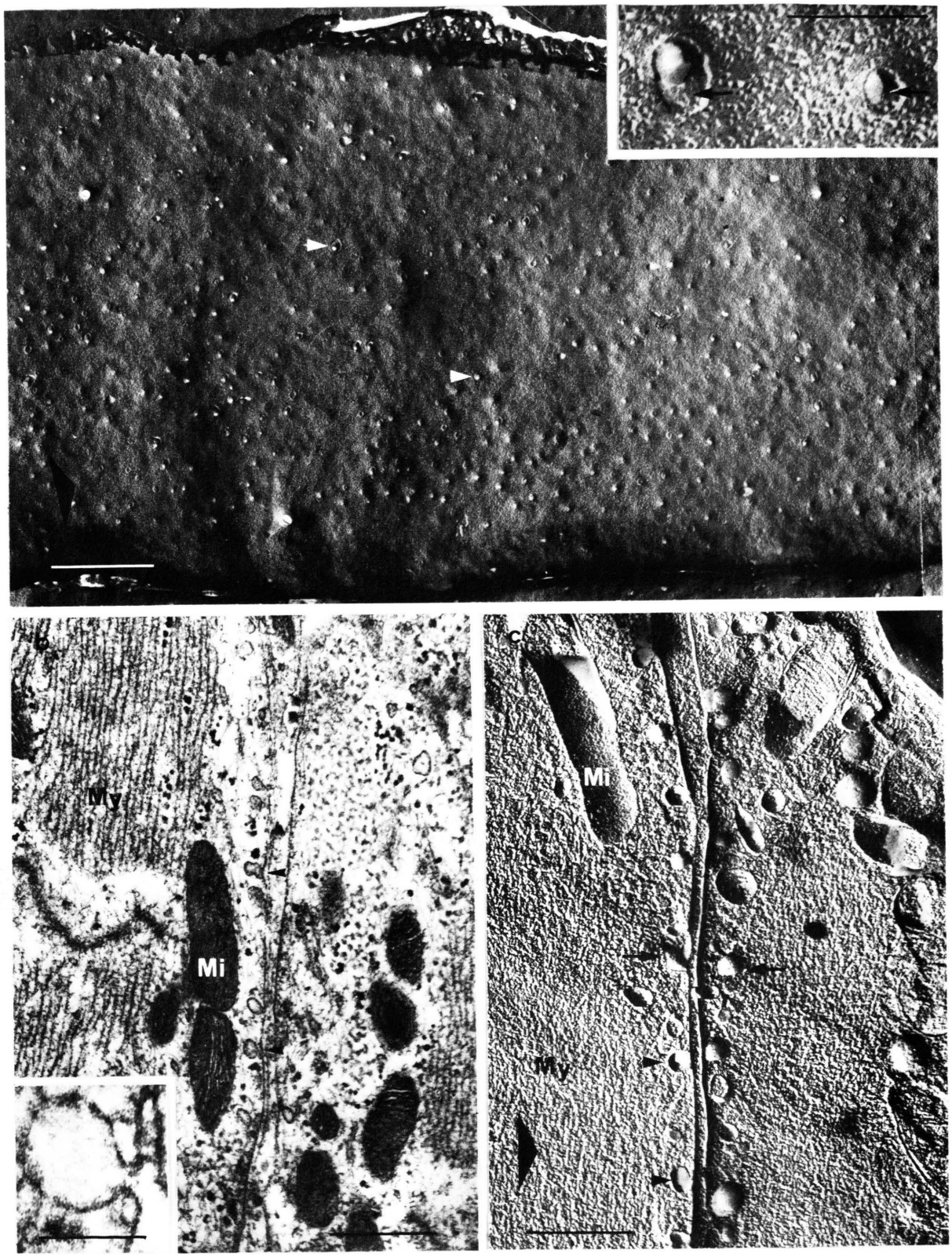

Fig. 1

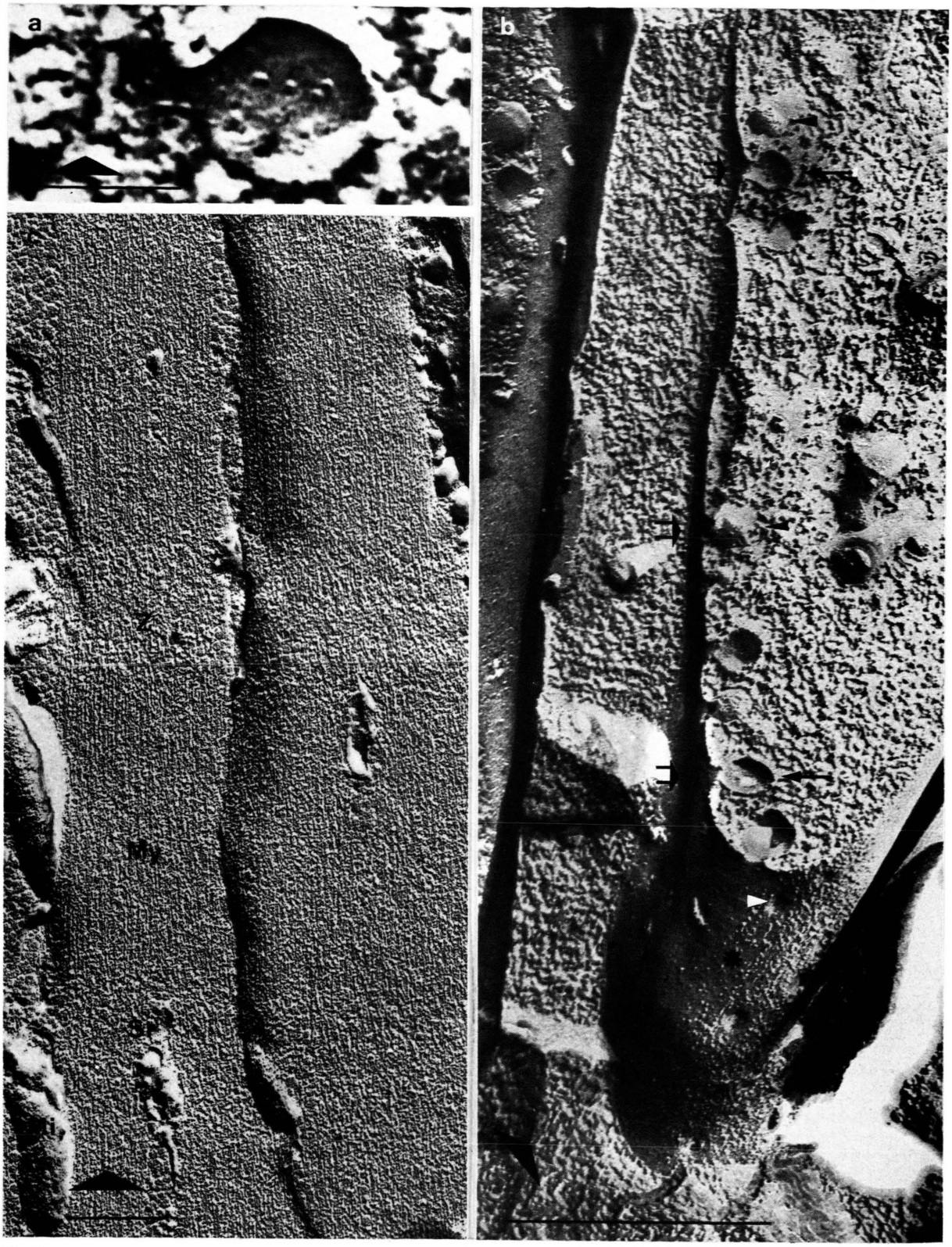

Fig. 2

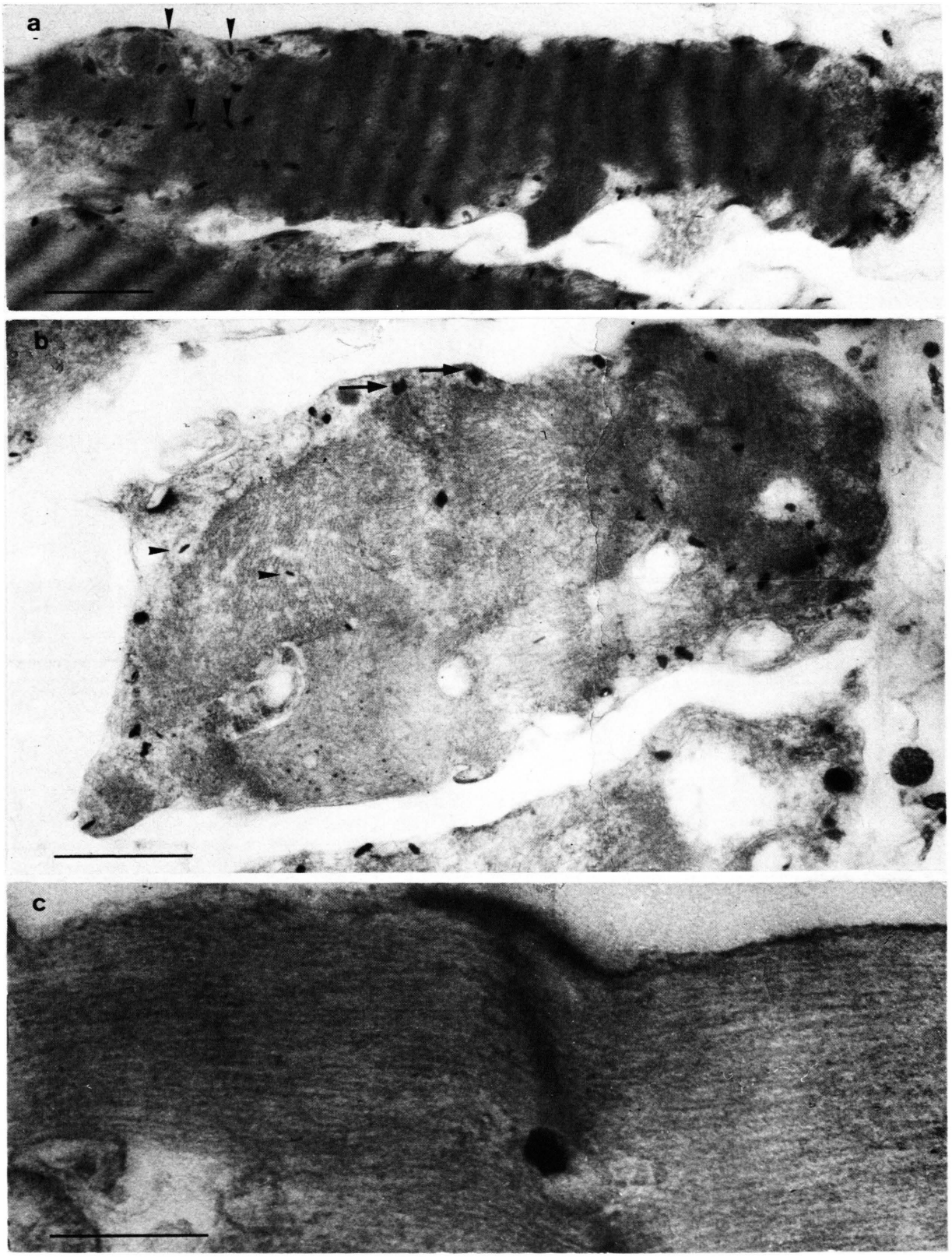

Fig. 3

spherical deposits measuring 150 nm in diameter and located within the metabolic center around the nucleus (Fig. 5a) as well as at the cell periphery between myofibrils and the plasma membrane (Fig. 4a, 5b). These deposits are identical with atrial granules always present in heart muscle cells of this type and not due to the preparation method used for the demonstration of an ATP-dependent Ca^{2+}-transport (see general morphology). (b) Longitudinal or elliptical deposits differing in size (long axis: 100–200 nm; diameter: 10–30 nm) and usually found in vesicles displayed immediately at the cell surface (Fig. 4a, b, arrow-heads and inset; 4c, d) or, to a lower extent, within intrafibrillar membranes of the sarcoplasmic reticulum (Fig. 3c). The membrane of the peripheral vesicles containing longitudinal deposits is often in continuity with the plasmalemma as described above for the caveolae-system (see general morphology).

Microprobe analysis of atrial granules from thin sections cut in the conventional way and floated on destilled water before they were mounted for evaluation deliver only a significant peak of osmium and phosphorus (Fig. 5i). In contrast, unconventionally cut sections prepared for analysis without contact to distilled water additionally contain considerable amounts of potassium (Fig. 5f).

Chemical composition of the longitudinal deposits within the caveolae-system and sarcoplasmic reticulum is rather different from that of atrial granules. X-ray spectra of sections cut with or without contact to water and analysed by scanning transmission electron microscopy (Fig. 6a–h) always deliver a significant peak of calcium (Fig. 6c, 6f). This demonstrates that the calcium in the longitudinal deposits is much stronger bound to the matrix than the potassium in the atrial granules.

Besides their molecular composition, shape, and cellular distribution the atrial granules differ from the longitudinal Ca^{2+}-containing deposits with respect to a high resistance against damages caused by the electron beam. After short times of stronger irridation the Ca^{2+}-containing deposits often completely dissappear thus leaving a whole in the plastics.

3. Control experiments

The generation and specification of Ca^{2+} containing deposits was investigated in more detail by different control experiments (see materials and methods). Incubation media without ATP or containing salyrgan as an ATPase-blocker were applied after fixation and before dehydration. Incubation without ATP largely depresses the formation of calcium-deposits, whereas salyrgan inhibits it completely (Fig. 5k). This demonstrates that the accumulation of Ca^{2+} within the caveolae-system and

---

Fig. 1. Freeze-fractured (a, c) and ultrathin-sectioned (b) bullfrog myocardial cells. Specimens were fixed with 1% OsO_4 and 2.5% glutaraldehyde. Mi, mitochondria; My, myofibrils; small arrowheads and arrows point to caveolae; big arrowhead indicates the direction of shadowing in a and c. a) Freeze-fracture replica showing PF of a myocardial cell. The randomly distributed indentations are openings of single caveolae (see also: Inset). Scale: 1 µm. Inset: IMP-distribution on PF of the sarcolemma. Around the necks of the caveolae a small area of ES is exhibited (arrows). Scale: 0.1 µm. b) Longitudinal section showing two neighbouring myocardial cells with a well-developed caveolae-system at the cell periphery. Scale: 0.5 µm. Inset: Medium sections demonstrate the continuity between the membrane of the caveolae and the sarcolemma. Scale: 0.1 µm. c) Longitudinal freeze-fracture through the cytoplasm of two neighbouring cells. The fracture plain reveals either PF (arrows) or EF (arrowheads) of caveolae. Same magnifications as b).

Fig. 2. Freeze-fractured bullfrog myocardial cells. Specimens were fixed with 2.5% glutaraldehyde (a, c) or with 1% OsO_4 and 2.5% glutaraldehyde (b). Mi, mitochondrium; My, myofibril; Z, Z-line; SR, sarcoplasmic reticulum; big arrowhead indicates the direction of shadowing. a) PF of a caveola with several large IMP (diameter: 8.4 nm). Scale: 0.1 µm. b) Replica exhibiting PF of the sarcolemma (star) with openings of caveolae (white arrowhead) and PF (arrows) as well as EF (arrow-heads) of crossfractured caveolae. IMP are visible on both, EF and PF of caveolae. Open connections between the caveola cavity and the extracellular space are marked by double arrows. Scale: 0.5 µm. c) Longitudinal fracture through the cytoplasm of a myocardial cell. A few elements of the sarcoplasmic reticulum are located inside the myofibrils (Sr). Scale: 0.5 µm.

Fig. 3. Histochemical demonstration of ATP-dependent Ca^{2+}-transport in bullfrog myocardial cells. Specimens were stabilized with 0.15% paraformaldehyde (a) or 50% glycerol (b, c). Arrowheads point to elliptical Ca^{2+}-deposits, arrows to atrial granules. a) Longitudinal section showing elliptical Ca^{2+}-deposits at the periphery and in the center of the cell. Scale: 1 µm. b) Cross section exhibiting atrial granules and elliptical Ca^{2+}-deposits. Scale: 1 µm. c) Longitudinal section through a myofibril. The Z-line contains a single SR-element with a Ca^{2+}-deposit. Scale: 0.5 µm.

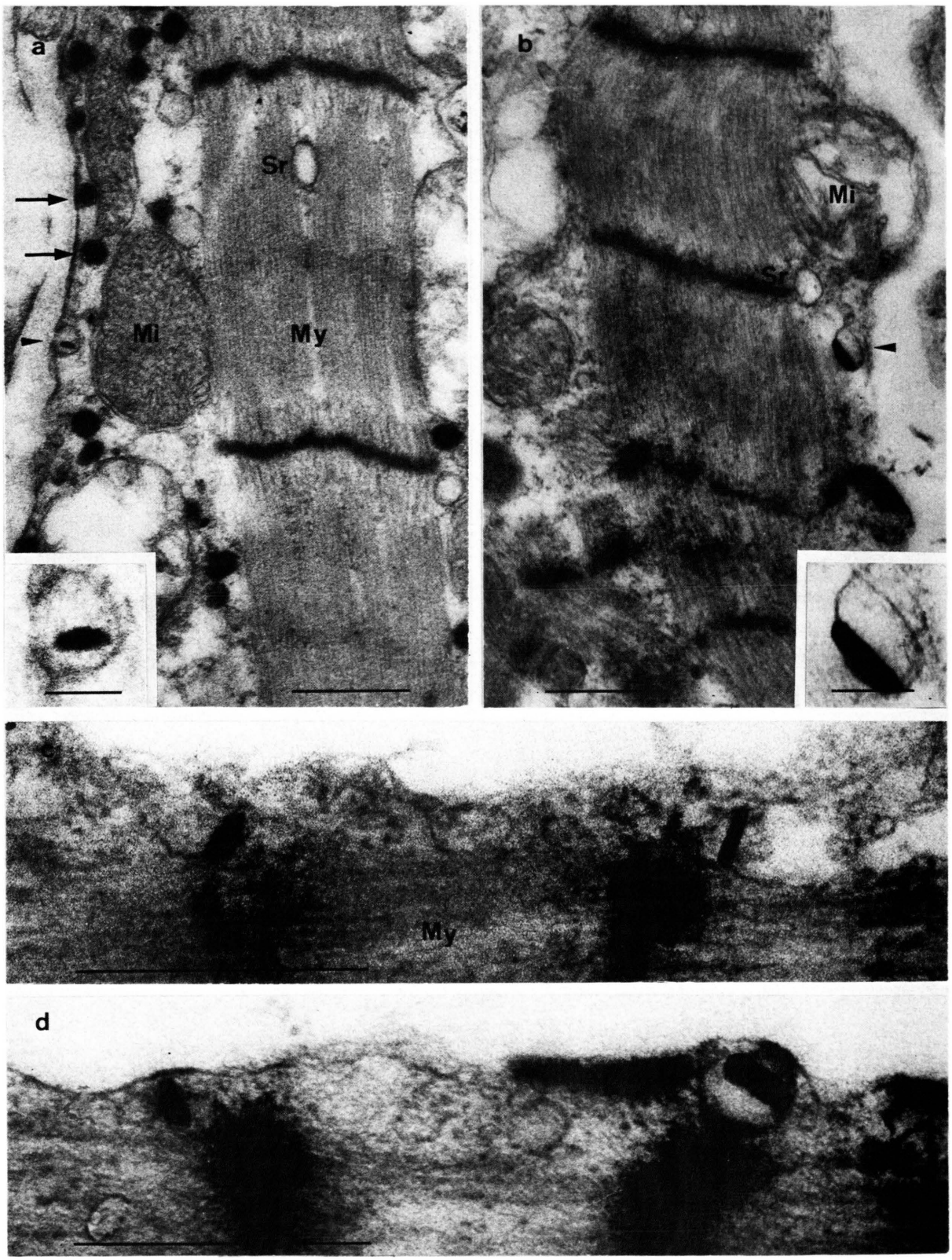

Fig. 4

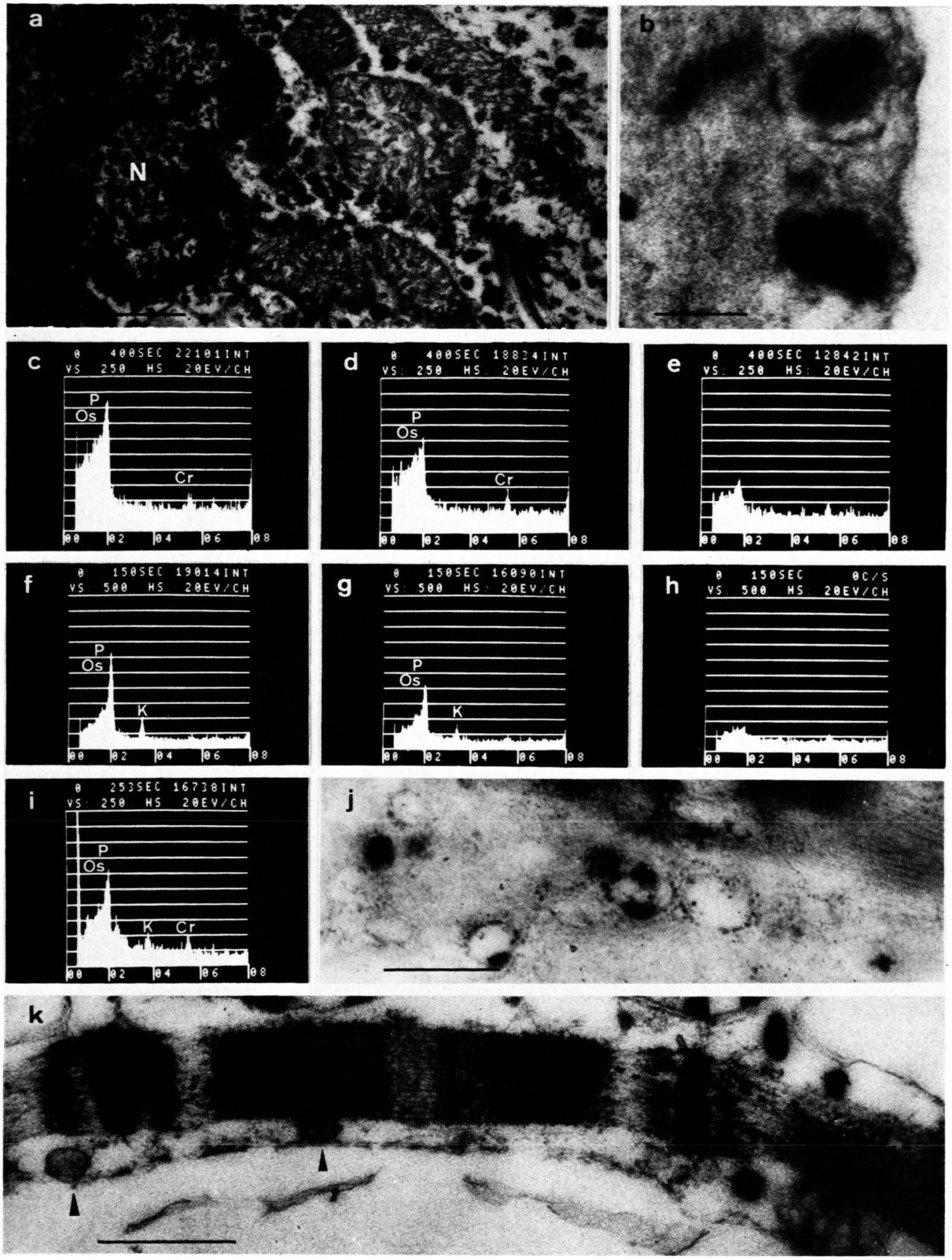
a
N
b
c
0 400SEC 22101INT
VS 250 HS 20EV/CH
P
Os
Cr
00 02 04 06 08
d
0 400SEC 18834INT
VS 250 HS 20EV/CH
P
Os
Cr
00 02 04 06 08
e
0 400SEC 12842INT
VS 250 HS 20EV/CH
00 02 04 06 08
f
0 150SEC 19014INT
VS 500 HS 20EV/CH
P
Os
K
00 02 04 06 08
g
0 150SEC 16090INT
VS 500 HS 20EV/CH
P
Os
K
00 02 04 06 08
h
0 150SEC 0C/S
VS 500 HS 20EV/CH
00 02 04 06 08
i
0 253SEC 16738INT
VS 250 HS 20EV/CH
P
Os
K Cr
00 02 04 06 08
j
k

Fig. 5

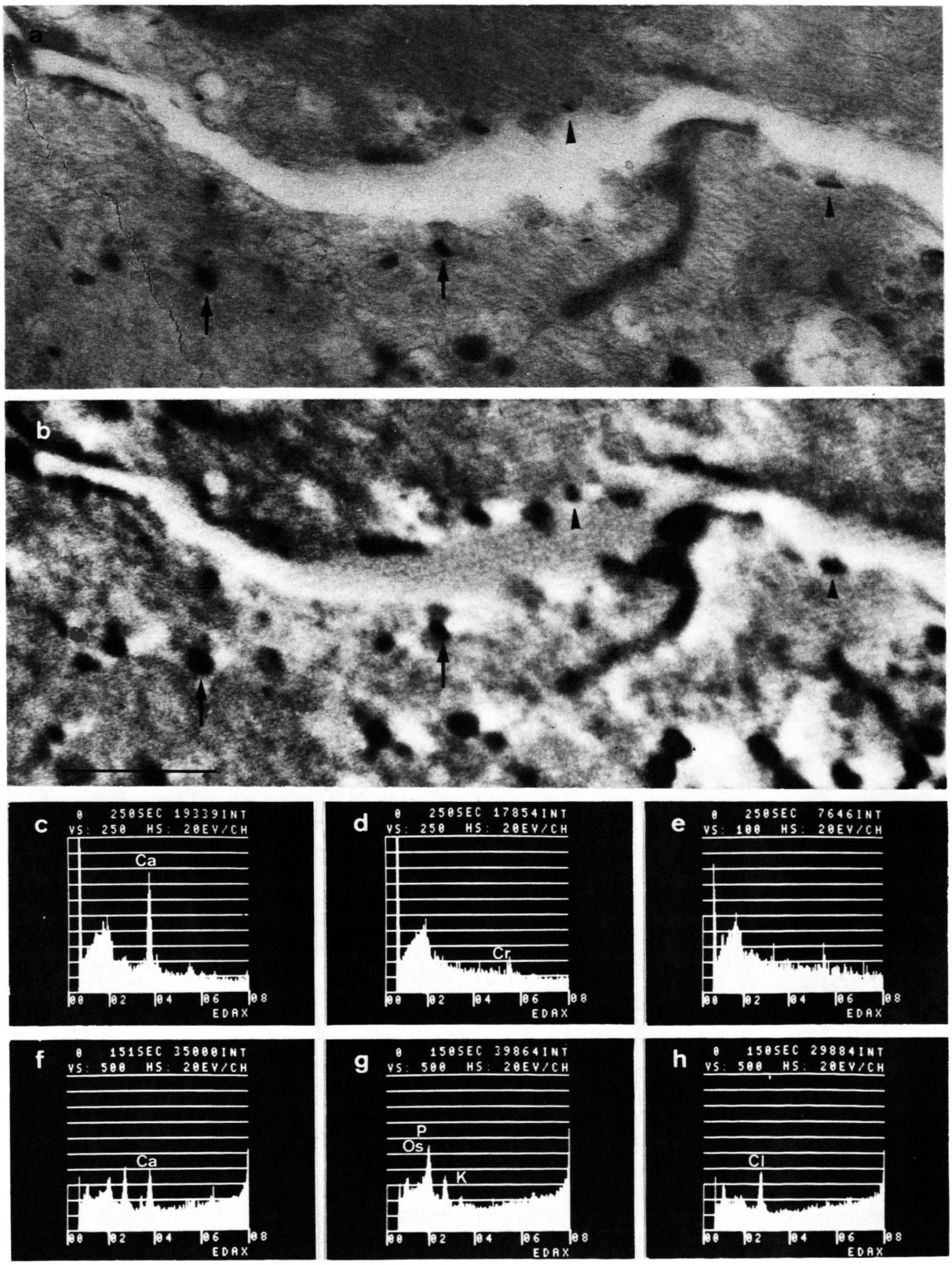
a
b
c
0 250SEC 19339INT
VS: 250 HS: 20EV/CH
Ca
00 02 04 06 08
EDAX
d
0 250SEC 17854INT
VS: 250 HS: 20EV/CH
Cr
00 02 04 06 08
EDAX
e
0 250SEC 7646INT
VS: 100 HS: 20EV/CH
00 02 04 06 08
EDAX
f
0 151SEC 35000INT
VS: 500 HS: 20EV/CH
Ca
00 02 04 06 08
EDAX
g
0 150SEC 39864INT
VS: 500 HS: 20EV/CH
P
Os
K
00 02 04 06 08
EDAX
h
0 150SEC 29884INT
VS: 500 HS: 20EV/CH
Cl
00 02 04 06 08
EDAX

Fig. 6

sarcoplasmic reticulum depends on ATPase-activity. Other specimens were incubated in 10^{-5} M ouabain solution to inhibit Na^+/K^+-ATPase-activity and thereby Na^+/Ca^{2+} countertransport. After this pretreatment calcium-deposits can be found in usual amounts and distribution, *i.e.* ouabain has no significant influence on calcium accumulation (Fig. 5j). To prove whether a Na^+-gradient is the energy-source for a Na^+/Ca^{2+} countertransport an incubation medium with high Na^+-concentration was tested. But incubation in 150 mM Na^+-solution failed to induce enrichment of calcium in any way.

Discussion

The results presented in this paper demonstrate the existence of an ATP-dependent Ca^{2+}-transport mechanism in two different cytoplasmic compartments of bullfrog atrial cells, *i.e.* in the so-called caveolae system and the sarcoplasmic reticulum (SR). The caveolae system is composed of numerous single membrane invaginations of spherical shape, which are randomly distributed at the entire cell periphery (see also, [16, 24, 25]). Multiple caveolae, as found in heart tissue of other species, *e.g.* carnivore papillary muscle [26] and skeletal muscle [14], were not observed in the bullfrog atrium. Since the membrane of most caveolae is continuous with the sarcolemma, the caveolae cavities open directly into the extracellular space.

Unlike the caveolae of skeletal muscle [14] and rabbit papillary muscle [25], those of bullfrog atrial cells are in possession of intramembraneous particles (IMP). The number and density of IMP in the caveolae membrane is significantly lower than in the sarcolemma. This is in good agreement with results on heart tissue of other species [16, 24] and on smooth muscle [15]. But contrary to smooth muscle the IMP of bullfrog atrial cells always show a regular distribution and are never accumulated around the neck-region of caveolae [15, 27, 28]. The diameter of the caveolae IMP in bullfrog atrial cells is larger than the average IMP-size in the sarcolemma. The measured value of 8.4 nm is comparable to the size of transport-enzymes such as Na^+/K^+-ATPase [29] and Ca^{2+}-ATPase of the SR [30] which were also determined in freeze-etch preparations.

According to the histochemical observations of this study the caveolae contain most of the Ca^{2+}-oxalate deposits formed during incubation. The opening between the caveolae cavity and the extracellular space does not seem to prevent accumulation and precipitation of Ca^{2+}. Although the low concentration of fixatives (see materials and methods) reveals an artifically increased number of caveolae, which have lost contact to the sarcolemma, Ca^{2+}-oxalate deposits were also found in open caveolae (*c.f.* Fig. 4a). The same observation was made in smooth muscle caveolae after precipitation experiments [31].

Fig. 4. Histochemical demonstration of ATP-dependent Ca^{2+}-transport in caveolae of bullfrog myocardial cells. Longitudinal sections of specimens, which were fixed with 0.025% glutaraldehyde (a), 50% glycerol (b, d), and 0.15% paraformaldehyde (c). My, myofibrils; Mi, mitochondria; SR, sarcoplasmic reticulum; arrowheads point to elliptical Ca^{2+}-deposits, arrows to atrial granules. a, b) Elliptical Ca^{2+}-deposits localized in single caveolae, partly in open connection with the extracellular space (see a, arrow-head and inset). Atrial granules are distributed between the myofibrils and the sarcolemma (a). Scale: 1 μm, inset 0.1 μm. c, d) Elliptical Ca^{2+}-deposits within single caveolae. Scale: 0.5 μm.

Fig. 5. Bullfrog myocardial cells. Atrial granules in histochemical preparations (a, b) and corresponding X-ray spectra (c – i). a) Numerous atrial granules around the nucleus (N); 0.15% paraformaldehyde. Scale: 1 μm. b) Atrial granules near to the sarcolemma; 50% glycerol. Scale: 0.1 μm. c – e) X-ray spectra of control-sections prepared without contact to water; 1% OsO_4 and 2.5% glutaraldehyde. c) Atrial granule; d) myoplasm; e) extracellular space. f – h) X-ray spectra of sections prepared without contact to water after histochemical treatment in incubation medium; 50% glycerol. f) Atrial granule; g) myoplasm; h) extracellular space. i) X-ray spectrum of an atrial granule in a section prepared with contact to water after histochemical treatment in incubation medium. For controls see Fig. 6 d and e. j, k) Histochemical control preparations; 0.15% paraformaldehyde. j) Specimen incubated in ouabain, elliptical Ca^{2+}-deposits are still present. Scale: 0.5 μm. k) Specimen incubated in salyrgan; arrowhead points to empty caveolae; atrial granules are present. Scale: 0.5 μm.

Fig. 6. a, b) Bullfrog myocardial cells in transmission (a) and scanning-transmission (b) electron micrographs of the same section-area with elliptical Ca^{2+}-deposits (arrowheads) and atrial granules (arrows); 50% glycerol; identical magnification. Scale: 0.5 μm. c–e) X-ray spectra of sections prepared with contact to water after histochemical treatment in incubation medium; 50% glycerol. c) Elliptical Ca^{2+}-deposits; d) myoplasm; e) extracellular space. f–h) X-ray spectra of sections prepared without contact to water after histochemical treatment in incubation medium; 50% glycerol. f) Elliptical Ca^{2+}-deposit; g) myoplasm; h) extracellular space.

From morphometrical calculations and measurements it can be concluded that most Ca^{2+}-oxalate deposits displayed in close vicinity to the sarcolemma belong to the caveolae system and not to the SR, because the total caveolae volume amounts to 8.5% and the SR volume only to 0.5% of the cell volume [5]. This means that the caveolae membrane of bullfrog atrial cells contains an ATP-dependent Ca^{2+}-pumping system as reported for smooth muscle [32] and mammalian heart sarcolemma [11]. Different control experiments were carried out to distinguish between such a Ca^{2+}-transport-ATPase and a possible Na^+/Ca^{2+} countertransport mechanism. According to these controls the demonstrated Ca^{2+}-accumulation in both, the SR and the caveolae system is not based on a Na^+/Ca^{2+} countertransport. At first glance this is surprising, since the existence of a coupled Na^+/Ca^{2+} exchange in heart muscle is well established and this mechanism is generally thought to be the main component of Ca^{2+}-outward-transport across the sarcolemma. However, there continues to be disagreement over the coupling ratios of Na^+/Ca^{2+} transport. An exchange of 2 Na^+ for 1 Ca^{2+} as proposed by Reuter and Seitz [33] cannot provide intracellular Ca^{2+}-levels below 20 μM [3]. To decrease intracellular Ca^{2+} below this level, as necessary for resting muscle, a coupling ratio of 4 Na^+: 1 Ca^{2+} must be postulated [3]. According to Chapman and Tunstall [34], the contractile responses of the frog heart are mostly consistent with an exchange of 3 Na^+ for 1 Ca^{2+}. If the original idea of a 2:1 coupling is maintained, one might argue that the Na^+/Ca^{2+} exchange is ATP-dependent in some way [35, 36] or the Na^+/Ca^{2+} exchange is supported by a second mechanism, *i.e.* and ATP-dependent Ca^{2+}-pumping system. Recent results of Carafoli [38] support the latter idea, because the Ca^{2+}-ATPase described by this author has a higher affinity to Ca^{2+} than the Na^+/Ca^{2+} counter-transport system. This view is consistent with the observation that a Na^+-lack contracture of frog heart muscle relaxes spontaneously within a few minutes although the Na^+/Ca^{2+} exchange remains blocked. It seems very likely that relaxation under these conditions is due to a Ca^{2+}-ATPase. Our results provide direct evidence that such a Ca^{2+}-ATPase is located at the membrane of the caveolae system in the bullfrog atrium.

Besides the caveolae system the SR represents a second cellular compartment concerned with active Ca^{2+}-transport. Although earlier experiments failed to demonstrate the existence of a Ca^{2+}-pumping system at the SR of amphibian heart tissue [5], the same structure has been shown to be able to accumulate Sr^{2+} [39]. This supports the results of the present paper. In the SR of mammalian heart tissue Ca^{2+}-stores have been described conclusively by antimonate precipitation [40], oxalate precipitation [41], and cryopreparations [42].

Finally, it should be mentioned that intracellular Ca^{2+}-pumping systems based on special ATPases are part of several theories for electro-mechanical coupling in myocardial cells, such as Ca^{2+}-induced Ca^{2+}-release in mammalian heart cells [43], Ca^{2+}-stores for the electro-neutral tonic tension [44] or caffeine-contracture in amphibian heart cells [45]. The demonstration of a Ca^{2+}-pumping mechanism bound to the caveolae system and the SR, now allows a better interpretation and understanding of these phenomena for bullfrog myocardium.

Acknowledgements

The authors thank Prof. Dr. W. Hasselbach and Prof. Dr. H. Komnick for helpful discussions of the results and U. Spies for technical assistance. This study was supported by the Deutsche Forschungsgemeinschaft and a fellowship of Konrad-Adenauer-Stiftung.

[1] W. Hasselbach, Fed. Proc. **23,** 909–912 (1964)
[2] R. A. Chapman, Prog. Biophys. Molec. Biol. **35,** 1–52 (1979).
[3] L. J. Mullins, Ion Transport in Heart, Raven Press, New York 1981.
[4] J. S. Sommer and E. A. Johnson, Z. Zellforsch. **98,** 437–468 (1969).
[5] S. G. Page and R. Niedergerke, J. Cell. Sci. **11,** 179–203 (1972).
[6] W. Hasselbach and M. Makinose, Biochem. Z. **333,** 518–528 (1961).
[7] A. Schwartz, M. L. Entman, K. Kaniike, L. K. Lane, W. B. van Winkle, and E. P. Bornet, Biochim. Biophys. Acta **426,** 57–72 (1976).
[8] H. C. Lüttgau and R. Niedergerke, J. Physiol. **143,** 486–505 (1958).
[9] H. Jundt, H. Porzig, H. Reuter, and J. W. Stucki, J. Physiol. **246,** 229–253 (1975).
[10] H. J. Schatzmann and F. F. Vincenzi, J. Physiol. **201,** 369–395 (1969).
[11] P. Caroni and E. Carafoli, Nature **283,** 765–767 (1980).
[12] L. Beaugé, R. DiPolo, L. Osses, F. Barnola, and M. Campos, Biochim. Biophys. Acta **644,** 147–152 (1981).
[13] A. H. Lichtman, G. B. Segel, and M. A. Lichtman, J. Biol. Chem. **256,** 6148–6154 (1981).
[14] A. F. Dulhunty and C. Franzini-Amstrong, J. Physiol. **250,** 513–539 (1975).
[15] G. Gabella and D. Blundell, Cell Tiss. Res. **190,** 255–271 (1978).
[16] M. Masson-Pévet, W. K. Bleeker, and D. Gros, Circ. Res. **45,** 621–629 (1979).
[17] S. Danneel and N. Weissenfels, Mikroskopie **20,** 89–93 (1965).
[18] A. R. Spurr, J. Ultrastruc. Res. **26,** 31–43 (1969).
[19] J. R. Sommer and W. Hasselbach, J. Cell. Biol. **34,** 902–905 (1967).
[20] H. G. Heumann, Protoplasma **67,** 111–115 (1969).
[21] K. M. Baldwin, J. Cell Biol. **46,** 455–476 (1970).
[22] M. Tarr and J. W. Trank, Experientia **32,** 338–340 (1976).
[23] J. R. Hume and W. Giles, J. Gen. Physiol. **78,** 19–42 (1981).
[24] G. Gabella, J. Ultrastruc. Res. **65,** 135–147 (1978).
[25] K. R. Levin and E. Page, Circ. Res. **46,** 244–255 (1980).
[26] W. G. Nayler and N. C. R. Merrillees, in: Calcium and the Heart, (P. Harris and L. Opie, eds.), pp. 24–65, Academic Press, London, New York 1971.
[27] C. E. Devine, F. O. Simpson, and W. S. Bertraud, J. Cell Sci. **8,** 427–443 (1971).
[28] L. Orci and A. Perrelet, Science **181,** 868–869 (1973).
[29] E. Skriver, A. B. Maunsbach, and P. L. Joergensen, J. Cell Biol. **86,** 746–754 (1980).
[30] W. Hasselbach, in: Topics in Current Chemistry **78,** pp. 3–55, Springer, Berlin, Heidelberg, New York 1979.
[31] L. M. Popescu, I. Diculescu, U. Zelck, and N. Ionescu, Cell Tiss. Res. **154,** 357–378 (1974).
[32] L. M. Popescu, in: Exitation Contraction Coupling in Smooth Muscle, (R. Casteels, T. Godfraind, and J. C. Rüegg, eds.), pp. 13–23, Elsevier, North Holland Biomedical Press, Amsterdam 1977.
[33] H. Reuter and N. Seitz, J. Physiol. **195,** 451–470 (1968).
[34] R. A. Chapman and J. Tunstall, J. Physiol. **305,** 109–123 (1980).
[35] L. J. Mullins and F. J. Brinley, J. Gen. Physiol. **65,** 135–152 (1975).
[36] C. Benninger, H. M. Einwächter, H. G. Haas, and R. Kern, J. Physiol. **259,** 617–645 (1976).
[37] R. DiPolo and L. Beaugé, Nature **278,** 271–273 (1979).
[38] E. Carafoli, Cell Calcium **2,** 353–364 (1981).
[39] S. Winegrad, J. Gen. Physiol. **62,** 693–706 (1973).
[40] M. J. Legato and G. A. Langer, J. Cell Biol. **41,** 401–423 (1969).
[41] I. Diculescu, L. M. Popescu, N. Ionescu, and N. Butucescu, Z. Zellforsch. **121,** 181–198 (1971).
[42] M. F. Wendt-Gallitelli, H. Wolburg, M. Schwegler, and W. Schlote, Experientia **35,** 1591–1593 (1979).
[43] A. Fabiato and F. Fabiato, J. Physiol. **249,** 469–495 (1975).
[44] H. M. Einwächter, H. G. Haas, and R. Kern, J. Physiol. **227,** 141–171 (1972).
[45] R. A. Chapman and J. Tunstall, J. Physiol. **316,** 30–31 P (1981).